Cancer Letters 613 (2025) 217500

Contents lists available at ScienceDirect

Cancer Letters

journal homepage: www.elsevier.com/locate/canlet

Original Articles

Combined MDM2 and G2/M checkpoint inhibition induces synergistic antitumor response in gastric signet-ring cell carcinoma

Dandong Luo [a,b,c,d,1], Huashe Wang [a,b,c,1], Jun Liu [b,c,e,g,1], Xiaochuan Chen [b,c,f,1], Yucheng Xu [b,c], Yufan Liang [b,c], Guannan Wang [b,c,h], Jiabo Zheng [a,b,c], Yonghe Chen [a,b,c], Xinyou Wang [a,b,c,***], Zhaoliang Yu [g,b,c,**], Lei Lian [a,b,c,*]

[a] Department of General Surgery (Gastric Surgery), The Sixth Affiliated Hospital, Sun Yat-sen University, Guangzhou, China
[b] Guangdong Provincial Key Laboratory of Colorectal and Pelvic Floor Diseases, The Sixth Affiliated Hospital, Sun Yat-sen University, Guangzhou, China
[c] Biomedical Innovation Center, The Sixth Affiliated Hospital, Sun Yat-sen University, China
[d] Department of Pathology, The First People's Hospital of Kashi Prefecture, Kashi, China
[e] Department of Clinical Laboratory, The Sixth Affiliated Hospital, Sun Yat-sen University, Guangzhou, China
[f] Department of Obstetrics and Gynecology, The Sixth Affiliated Hospital, Sun Yat-sen University, Guangzhou, China
[g] Department of General Surgery (Colorectal Surgery), The Sixth Affiliated Hospital, Sun Yat-sen University, Guangzhou, China
[h] Department of Pathology, The Sixth Affiliated Hospital, Sun Yat-sen University, Guangzhou, China

ARTICLE INFO

Keywords:
Signet-ring cell carcinoma
MDM2 inhibitor
WEE1 inhibitor
Synergistic effects

ABSTRACT

Signet ring cell carcinoma (SRCC) poses a considerable challenge in terms of treatment, given its refractory nature and poor outcomes. Unlike other cancers, SRCC exhibits significant MDM2 copy number gains, with elevated MDM2 expression linked to poor prognosis. MDM2 inhibition induces a morphological transition in SRCC cells by suppressing E-cadherin degradation, which may render these cells vulnerable to a second drug. Using a high-throughput drug screen, our study demonstrated that the combination of MDM2 inhibitors with G2/M checkpoint inhibitors, including WEE1 or CHK1 inhibitors, can elicit a synergistic antitumor response in SRCC cells by inducing DNA damage. Furthermore, pharmacological inhibition of MDM2, WEE1, or CHK1 significantly impeded tumor growth in *in vivo* mouse models and organoids of SRCC. Collectively, our findings indicate that MDM2 inhibition-induced morphological changes may enhance the efficacy of G2/M checkpoint inhibitors, presenting a promising combined treatment for SRCC.

1. Introduction

The treatment of signet ring cell carcinoma (SRCC) poses a major challenge because of its resistance to chemotherapy, and its unfavorable prognosis [1]. SRCC is characterized by distinct physical features of signet ring cells, commonly found in various solid tumors, such as gastric cancer (GC) [2]. Gastric SRCC is observed in younger individuals, women, and the lower stomach regions [3]. In recent years, the frequency of SRCC consistently increased, comprising 35 45 % of GC cases [4]. Currently, chemotherapy is the main form of therapy, and there are no targeted drug therapies for SRCC [5]. Hence, the development of new and effective drug treatments is urgently required.

Genetic variations can potentially account for SRCC traits. *TP53* and *CDH1* mutations are frequently observed in SRCC, and high-frequency amplification of several oncogenes, such as *FGFR2*, *MYB*, and *MDM2,* are characteristic of SRCC [6]. Patients with SRCC harboring CLDN18-ARHGAP26/6 fusions have poor prognoses and do not respond well to oxaliplatin/fluoropyrimidine chemotherapy [7]. This unique genetic variation could potentially account for many of the SRCC traits. SRCC stands out because of the existence of goblet-like cytoplasmic

* Corresponding author. Department of General Surgery (Department of Gastric Surgery), The Sixth Affiliated Hospital, Sun Yat-sen University, 26 Yuancun Er Heng Rd. Guangzhou, Guangdong, China.
** Corresponding author. Biomedical Innovation Center, The Sixth Affiliated Hospital, Sun Yat-sen University, China.
*** Corresponding author. Department of General Surgery (Gastric Surgery), The Sixth Affiliated Hospital, Sun Yat-sen University, Guangzhou, China.
E-mail addresses: wangxy365@mail.sysu.edu.cn (X. Wang), yuzhaol@mail2.sysu.edu.cn (Z. Yu), lianlei2@mail.sysu.edu.cn (L. Lian).
[1] These authors contributed equally to this work.

https://doi.org/10.1016/j.canlet.2025.217500
Received 19 May 2024; Received in revised form 17 January 2025; Accepted 22 January 2025
Available online 31 January 2025

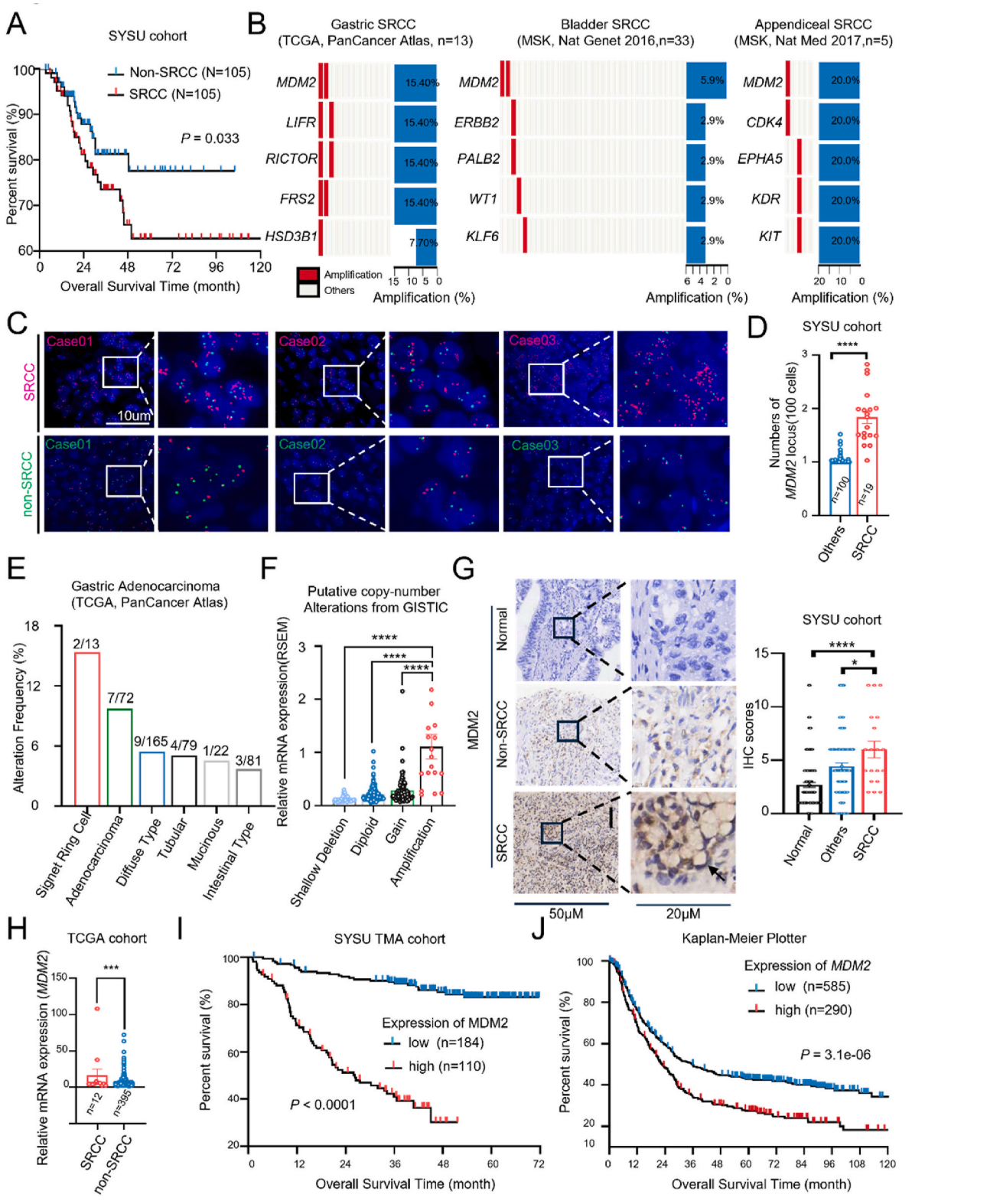

(caption on next page)

Fig. 1. Copy number gains of *MDM2* are a critical characteristic of SRCC, and high MDM2 expression correlates with poor prognosis (A) The Kaplan-Meier curves of overall survival (OS) in SYSU cohort patients grouped according to SRCC status. (B) CNV gene frequency of SRCC in the stomach, bladder, and appendix. (C and D) Representative images (C) and quantification (D) of FISH demonstrating the MDM2 locus in SRCC (n = 19) and other types of GC (n = 100) from the SYSU cohort have been presented. The images have been color-coded, with blue representing DNA stained with DAPI, green representing the centromere of chromosome 12, and red representing the genomic locus of MDM2 (Scale bars, 2 μm), Mann-Whitney *U* test was applied. (E) Genetic alteration frequency of MDM2 in each pathological subtype in TCGA-STAD cohort. Each group represents the proportion of gastric cancer patients with MDM2 gene abnormality in this pathological subtype. (F) The mRNA expression of MDM2 according to different MDM2 amplification status (Shallow Deletion, Diploid, Gain and Amplification). (G) Representative immunohistochemical staining (IHC) images of MDM2 in gastric SRCC (n = 19), other types of GC (n = 100), and normal stomach tissues (n = 100) from SYSU (The Sixth Affiliated Hospital of Sun Yat-sen University) cohort (Left) (Scale bar, 20 μm). IHC scores of MDM2 in gastric SRCC (n = 19), other types of GC (n = 100), and normal stomach tissues (n = 100) (Right), the Mann-Whitney *U* test was performed. (H) The Mann-Whitney *U* test was performed to compare the mRNA expression of MDM2 between patients with scirrhous gastric cancer (SRCC) (n = 12, shown in red) and other types of gastric cancer (GC) patients (n = 395, shown in blue) from the TCGA-STAD cohort. (I) The Kaplan-Meier curves of OS in the SYSU-TMA cohort grouped according to high (red, n = 110) and low (blue, n = 184) MDM2 expression. (J) The Kaplan-Meier curves of OS in GC cohort from Kaplan-Meier Plotter Database grouped according to high (red, n = 290) and low (blue, n = 585) MDM2 expression. (For interpretation of the references to color in this figure legend, the reader is referred to the Web version of this article.)

mucin and nuclei that are displaced in an eccentric manner. *CDH1* encodes E-cadherin, an essential molecule for cell adhesion in SRCC formation. The absence of E-cadherin is regarded as a vital factor in the cellular transition from epithelial to mesenchymal and is linked to resistance to treatment [8–10]. Hence, it is plausible to consider therapies based on genomic features or the morphological plasticity of SRCC.

The activities of p53 are mediated by MDM2, which facilitates its degradation [11]. Overexpression and amplification of MDM2 can accelerate the tumor growth [12]. The MDM2 inhibitor Nutlin-3 (Nut) has demonstrated activity in preclinical studies, and another MDM2 inhibitor, idasanutlin (Ida), has shown antitumor activity and safety in clinical trials [13].

Our study suggests that SRCC can be distinguished based on *MDM2* amplification and elevated MDM2 expression. Moreover, MDM2 inhibitors altered the appearance of SRCC cells from a s signet ring-like shape to a spindle-like shape by enhancing the expression of E-cadherin. Synergistic lethal effects can be induced in SRCC by activating p53 expression and triggering the DNA damage response through G2/M checkpoint inhibitors, such as WEE1 and CHK1 inhibitors, in combination with MDM2 inhibitors. This study presents a potentially effective therapeutic approach for SRCC, thereby offering potential enhancements in patient prognosis.

2. Results

2.1. Copy number gains of MDM2 are a critical characteristic of SRCC and higher MDM2 expression correlates with poor prognosis

SRCC exhibits a decreased therapeutic response rate and worse prognosis than those of other types of GC [3]. A correlation between SRCC and reduced overall survival was identified in the SYSU cohort, as well as in the TCGA-STAD and ACRG (GSE62254) cohorts (Fig. 1A and S1A–D). To determine the essential copy number variations (CNV) genes in SRCC, we extracted genomic data from the cBioPortal database. *MDM2* is frequently altered in gastric, bladder, and appendiceal cancers (Fig. 1B). MDM2, an E3 ubiquitin ligase, plays a crucial role in promoting the degradation of the p53 protein [14]. To confirm the impact of MDM2 amplification in SRCC, we performed further studies utilizing in situ fluorescence hybridization (FISH) and immunohistochemistry (IHC) in practical scenarios. FISH analysis was conducted on 19 SRCC cases and 100 cases of different forms of GC to examine *MDM2*. In SRCC cases, FISH analysis revealed significant amplification of *MDM2* when compared with that in other types of GC (Fig. 1C–D). The prevalence of *MDM2* changes exceeded 6 % in GC, whereas it was 2/13 (15.4 %) in SRCC (Fig. 1E and S1I). The alteration frequency of *MDM2* in colorectal cancer was lower than that in GC (Fig. S1H). Furthermore, an increased CNV of *MDM2* was significantly associated with *MDM2* transcript abundance (Fig. 1F). These results imply that amplification of *MDM2* could be a pathogenic event in a subgroup of SRCC.

MDM2 expression was significantly higher in SRCC than in other GC types or para-carcinoma tissues (Fig. 1G). Moreover, in the TCGA-PanCancer-Atlas cohort, the alteration frequency of *MDM2* in colorectal cancer was lower than that in GC (Fig. S1H). IHC of tissue microarray from the SYSU and GEPIA2 cohorts revealed a significant increase in MDM2 levels in GC tumors compared to para-carcinoma ($P < 0.05$, Figs. S1E–F) [15]. Moreover, there was a notable link between elevated MDM2 levels and reduced duration of both overall survival and progression-free survival in the SYSU cohort and Kaplan–Meier Plotter database ($P < 0.05$, Fig. 1I–J and S1G) [16]. Our study enhances the understanding of *MDM2* amplification in SRCC, suggesting its potential as a key biomarker and therapeutic target.

2.2. Inhibition of MDM2 suppresses E-cadherin degradation in SRCC cells independent of TP53 status

To evaluate the cytotoxic effects of MDM2 inhibitors (Nut; Ida) on GC in *vitro*, colony formation and growth curve assays showed that cell lines derived from SRCC, including SNU668, KATOIII, and NUGC3 with poor differentiation, exhibited significant resistance to MDM2 inhibitors (Fig. 2A and B). The tumorsphere formation assay revealed the same results (Figs. S2A–B). Cells resistant to MDM2 inhibitors, including SNU668, KATOIII, NUGC3, and MKN74, showed elevated MDM2 expression levels (Figs. S2C–D). The CCLE public database was used to further investigate the sensitivity of MDM2 inhibitors to SNU668 and NUGC3. The survival rates of NUGC3 and SNU668 cells treated with the same dose of MDM2 inhibitor were significantly higher compared than those of MKN45 and AGS cells (Fig. S2E) [17]. Although MDM2 inhibitor monotherapy proved ineffective in SRCC cells, it induced a spindle-shaped morphology *in vitro* (Fig. 2D). The SNU668-xenograft model, when treated with an MDM2 inhibitor, also exhibited a transformation resembling a spindle (Fig. 2E). The inhibition of MDM2 caused a notable decrease in the cell cycle, but it did not trigger apoptosis (Fig. 2C and S2F). MDM2 is a key negative regulator of p53, but evidence indicates its oncogenic functions also operate independently of p53 [13,21,22]. We found that p53 expression increased in *TP53* wild-type cells (SNU638 and MKN45) and was stable in *TP53* mutant cells (NUGC3 and KATOIII) after treatment with MDM2 inhibitors (Fig. 2G), indicating that MDM2 inhibition may affect SRCC cells independently of p53.

Our analysis revealed that MDM2 amplification and p53 status are not significantly correlated in public databases, suggesting that MDM2 amplification or high expression might be crucial in *TP53* mutant tumors (Fig. S3A). This implies an independent aberrant expression pattern of *MDM2* unrelated to *TP53* status. Furthermore, tumors with high *MDM2* expression and *TP53* mutations exhibited the worst progression free survival in multiple cancers (Fig. S3B). These data suggest that *MDM2* may play an oncogenic role in *TP53* mutant tumors, which supports our findings in SRCC.

The lack of E-cadherin expression is a key feature of SRCC, indicating that E-cadherin may contribute to transformational plasticity.MDM2-mediated posttranscriptional changes in breast cancer suggest that MDM2 may lead to decreased E-cadherin expression [9,18,19]. We

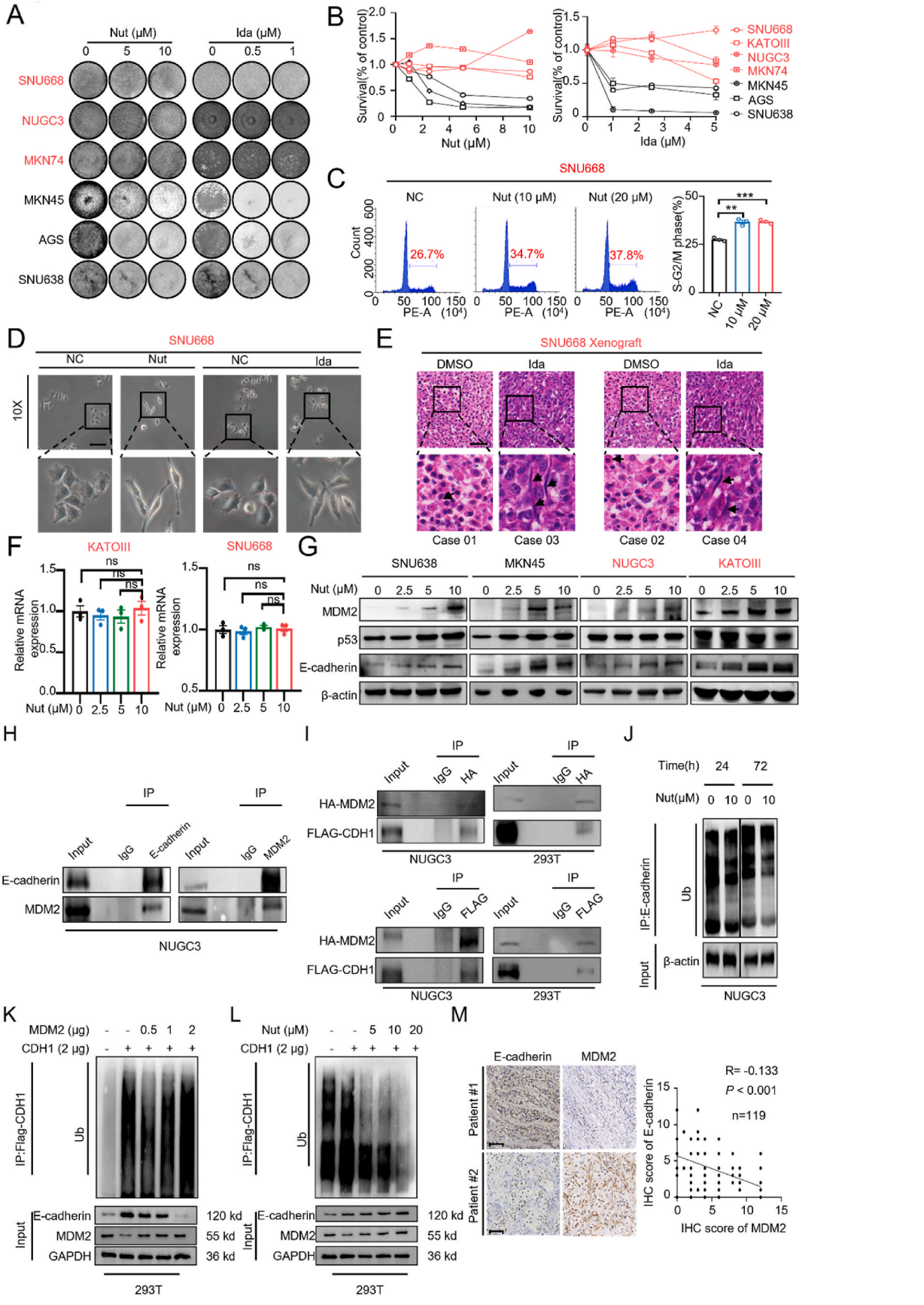

(caption on next page)

Fig. 2. Inhibition of MDM2 suppresses E-cadherin degradation in SRCC cells. (A) Representative image of the colony formation assay in GC (Gastric cancer) cells treated with MDM2 inhibitors (Nutlin, Nut; Idasnutlin, Ida) for 8 days. (B)The viability of GC cells treated with Nut and Ida for 4 days. (C) The cell cycle analysis on SNU668 treated with Nut for 48 h. Left panel, representative images of fluorescence-activated cell sorting (FACS) analysis, right panel, S-G2/M phase. (D) The representative image of cell morphology of SNU668 treated with Nut (15 μM) and Ida (10 μM) for 24 h (Scale bar, 100 μm). (E) The representative hematoxylin and eosin (H&E) staining image of SNU668 -xenograft model mice treated with (Case 03 and 04) or without Ida (Case 01 and 02) (37.5 mg/kg) (Scale bar, 20 μm). (F) RT-qPCR assay of SRCC cell lines treated with Nut for 24 h. (G) Western blot assay of resistant GC cells (NUGC3 and KATOIII) and sensitive GC cells (SNU638 and MKN45) treated with Nut at the indicated time points (NUGC3 and KATOIII, 72 h; SNU638 and MKN45, 24 h). (H) The co-immunoprecipitation (Co-IP) analysis of endogenous platelet proteins reveals that MDM2 specifically associates with E-cadherin in NUGC3 cells. Immunoglobulin G (IgG) was employed as a control. (I) The Co-IP assay was conducted in 293T and NUGC3 cells following transfection of the overexpressed CDH1 plasmid labeled with FLAG and MDM2 labeled with HA, respectively. (J) The ubiquitination levels were assessed in NUGC3 cells treated with Nut and subjected to Co-IP analysis incubating E-cadherin. (K) The ubiquitination coimmunoprecipitation and Western blot were performed in 293T cells treated with an overexpression plasmid FLAG-CDH1, either alone or in combination with the overexpression plasmid HA-MDM2. (L) The ubiquitination coimmunoprecipitation and Western blot were conducted in 293T cells treated with an overexpression plasmid FLAG-CDH1, either alone or in combination with the MDM2 inhibitor Nut. (M) Representative immunohistochemical staining (IHC) images of E-cadherin and MDM2 in GC tissues (Left) (Scale bar, 20 μm). Relationship between E-cadherin and IHC scores of MDM2 in GC tissue (n = 119) (Right).

hypothesized that elevated MDM2 levels inhibit E-cadherin expression in SRCC. Inhibiting MDM2 increased E-cadherin expression and altered SRCC morphology. Inhibition of MDM2 did not significantly alter CDH1 mRNA expression (Fig. 2F). Interestingly, the gradual upregulation of E-cadherin was dependent on the concentration of Nut (Fig. 2G). We further examined whether MDM2 directly interacted with E-cadherin and aided in posttranscriptional regulation. Endogenous E-cadherin was identified in the anti-MDM2 immunoprecipitate, with this interaction validated through reciprocal immunoprecipitation and immunoblotting (Fig. 2H and I). Nut treatment also decreased E-cadherin ubiquitination levels (Fig. 2J). E-cadherin ubiquitination increased with MDM2 and CDH1 overexpression but decreased dose-dependently with higher Nut concentrations (Fig. 2K and L). Previous studies have also supported that MDM2 can induce protein ubiquitination and regulate cells independently of p53 [20–22]. Mechanistically, MDM2 directly binds to E-cadherin and induces its ubiquitination.

The findings suggest an interaction between MDM2 and E-cadherin. The study found a significant negative correlation between the IHC intensities of MDM2 and E-cadherin in SRCC ($P < 0.001$, $R = -0.3647$) (Fig. 2M). Nut sensitivity showed a negative correlation with both MDM2 copy number and expression, while it was positively correlated with E-cadherin levels (Figs. S4A–C). The findings corroborate the theory that MDM2 disrupts E-cadherin expression, leading to the transformation of SRCC cells into a signet ring-like morphology.

2.3. Combined MDM2 inhibitors with G2/M checkpoint inhibitors can induce a synergistic antitumor effect on SRCC in vitro

After observing the capacity of MDM2 inhibition to cause cell cycle arrest in SRCC, we examined the potential for combining drugs targeting the cell cycle apparatus along with MDM2 inhibition. Candidate drugs can be effectively selected using high-throughput drug screening combined with the detection of a combination index [23]. First, we examined 130 compounds that inhibited the kinases involved in the cell cycle in SNU668 cells (Supplementary Tables 1–2). Through drug screening, we assessed the effects of Nut (15 μM) in combination with kinase inhibitors (0.2 μM). Notably, 15 potential compounds were identified, and five of them demonstrated inhibitory effects on the G2/M phase checkpoint, such as CHK1 and WEE1 inhibitors (Fig. 3A and B). Combination index analysis showed a collaborative connection between Nut and either adavosertib (Ada, a WEE1 inhibitor) or PF477736 (a CHK1 inhibitor) (Fig. 3C). This combined effect was also confirmed by colony formation and growth histogram assays (Fig. 3D and E). Furthermore, the knockdown of *MDM2* induced spindle-shaped morphology and caused coordinated lethality with G2/M checkpoint inhibitors in the SNU668 cells (Figs. S5A–C). Cancer stem cells are a small group of tumor cells with exceptional self-renewal and differentiation abilities. They play pivotal roles in tumor initiation and perpetuation, while concurrently exhibiting chemoresistance and fostering tumor progression [24–26]. The combination therapy was found to effectively inhibit the cancer stem cells of SRCC, as demonstrated by the tumorsphere assay. This suggests that implementing this modified strategy may lead to a reduction in tumor recurrence (Fig. 3F–G and S5D–E). Combination therapy significantly elevated phosphorylated histone H2AX expression (Fig. 3H–K and S5F–H). These results show that the combination of MDM2 inhibitors with G2/M checkpoint inhibitors can induce a synergistic antitumor effect on SRCC *in vitro*.

2.4. Combination of MDM2 inhibitor and G2/M checkpoint inhibitors induces a synergistic antitumor effect in vivo and ex vivo

An NUGC3-derived xenograft nude mouse model was used to evaluate the synergistic effects in vivo. While Ida monotherapy had no effect and Ada monotherapy only had a modest effect on reducing tumor growth, the combination of Ida and Ada significantly suppressed tumor growth (Fig. 4A–C). The weight of mice in the combination group decreased (Fig. 4D and K), which may be due to the low weight of the xenograft tumors in the combination group (Fig. 4D and K). This study indicates that combination therapy significantly reduced Ki-67 levels and elevated cleaved caspase-3 levels (Fig. 4E–G). Additionally, substantial combination inhibition was confirmed in the SNU668-derived xenograft nude mouse model (Fig. 4H–N and S6A–E). Liquid chromatography-mass spectrometry was used to measure plasma drug concentrations in BALB/c nude mice treated with Ida and Ada for 3 h. Results showed a significant increase in concentration in the Ida and Ada groups compared to the negative control group (Figs. S6F–K). WEE1 kinase phosphorylates the cell division cycle (CDC2) gene, downregulating its activity and thereby regulating the G2 to M phase transition and mitosis [24,25]. Therefore, we examined phosphorylated CDC2 as a marker of WEE1 inhibition. IHC was performed to investigate the systemic effects of Ida and Ada. In the combination group, phosphorylated CDC2 expression notably decreased, while MDM2 expression significantly increased (Fig. 4O–Q).

Patient-derived organoids (PDOs) are cutting-edge research models that accurately replicate the original tissue's phenotypic and genetic characteristics, proving essential for disease study and drug screening [26]. We confirmed the clinical efficacy of this combination strategy using a PDO model. A patient who underwent preoperative neoadjuvant therapy consisting of four cycles of a PD-1 inhibitor and FLOT regimens was used to establish an SRCC-derived organoid (SRCC-1099) (Fig. 5A). SRCC-1099 organoids were derived from patients with SRCC, whereas GC-1097 organoids were derived from the diffuse type of adenocarcinoma with poor differentiation (Supplementary Table 3). However, after analyzing the imaging and pathological results before and after treatment, the tumors did not show a significant decrease (Fig. 5B and C). Histopathological examination confirmed the establishment of SRCC-1099 using IHC (Fig. 5D). MDM2 expression was positively identified in tissues and organoids derived from PDO (Fig. S6L). The simultaneous application of an MDM2 inhibitor with a WEE1 or CHK1 inhibitor effectively inhibited SRCC-1099 progression (Fig. 5E). The effectiveness of the MDM2 inhibitor in conjunction with a G2/M checkpoint inhibitor was validated using the GC-1097 organoid model,

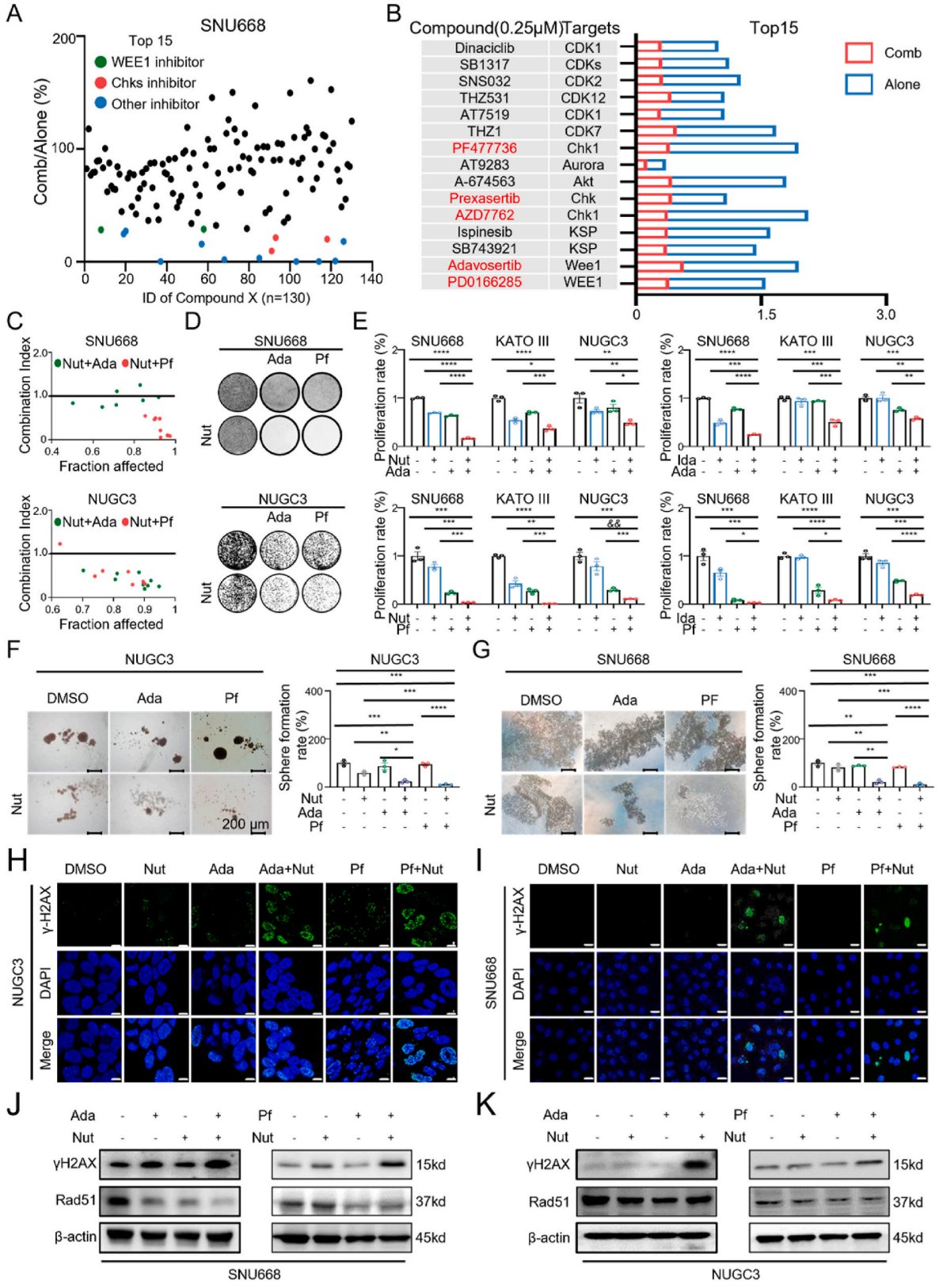

(caption on next page)

Fig. 3. Combined MDM2 inhibitors with G2/M checkpoint inhibitors can induce a synergistic antitumor effect on SRCC in vitro (A) The combinatorial effects of 130 inhibitors related to the cell cycle in SNU668 were evaluated. Each data point represents the normalized cell viability (Combination/Nut) after treatment with compound X (0.2 μM), either alone or in combination with Nut (15 μM). The non-black data points correspond to the top 15 most effective drugs, including WEE1 inhibitors (green), Chks inhibitors (red), and another inhibitor (blue). (B) The accompanying histogram and table depict the survival rate (Combination/Nc or monotherapy alone/Nc) of SNU668 cells treated with the 15 most potent drugs (0.2 μM), either individually or in combination with Nut (15 μM), over a duration of 6 days. (C) The drug combination index (CI) was determined for Nut and Ada/Pf in SNU668 and NUGC3 cells using a cell survival assay at 6d. The CI values were interpreted as follows: CI < 1 indicated17 synergism, CI $= 1$ indicated additivity, and CI > 1 indicated antagonism. (D) The representative image of colony formation assay of SNU668 and NUGC3 cells treated with Nut, Ada, Pf, or a combination of these drugs after 12 days. (E) The growth histogram of SNU668, KATOIII, and NUGC3 cells treated with Nut or Ida in combination with Ada or Pf at the indicated concentrations (SNU668: Nut 15 μM, Ida 5 μM, Ada 0.2 μM, Pf 0.2 μM; KATOIII: Nut 10 μM, Ida 5 μM, Ada 0.1 μM, Pf 0.1 μM; NUGC3: Nut 10 μM, Ida 2 μM Ada 0.1 μM, Pf 0.1μ M) was analyzed over a period of 6 days. (F) The left panel displays the representative image of tumor sphere formation assay in NUGC3 cells treated with Nut, Ada, Pf, or a combination of these compounds at specified concentrations (Nut 10 μM, Ada 0.2 μM, Pf 0.2 μM) for a duration of 10 days (Scale bar: 200 μm). The right panel shows the relative rate of tumor sphere formation. (G) The left panel displays the representative image of tumor sphere formation assay in SNU668 cells treated with Nut, Ada, Pf, or a combination of these compounds at specified concentrations (Nut 10 μM, Ada 0.25 μM, Pf 0.25 μM) for a duration of 10 days (Scale bar: 200 μm). The right panel shows the relative rate of tumor sphere formation. (H) The representative image of γ-H2AX staining in NUGC3 cells treated with Nut, Ida Ada, Pf or a combination at the indicated concentrations (Nut 1 μM, Ada 0.25 μM, Pf 0.025 μM) for 72 h. (I) The representative image of γ-H2AX staining in SNU668 cells treated with Nut, Ida Ada, Pf or a combination at the indicated concentrations (Nut 10 μM, Ada 0.25 μM, Pf 0.025 μM) for 72 h. (J) The SNU668 cells were subjected to Western blot analysis after treatment with Nut, Ada, Pf, or a combination of these compounds at specified concentrations (Nut 10 μM, Ada 0.25 μM; Pf 0.025 μM) for a duration of 4 h. (K) The NUGC3 cells were subjected to Western blot analysis after treatment with Nut, Ada, Pf, or a combination of these compounds at specified concentrations (Nut 10 μM, Ada 0.25 μM; Pf 0.25 μM) for a duration of 4 h. (For interpretation of the references to color in this figure legend, the reader is referred to the Web version of this article.)

derived from poorly differentiated gastric adenocarcinoma (Fig. 5F and G). The combination of the MDM2 inhibitor with G2/M checkpoint inhibitors effectively inhibited SRCC growth both in vivo and ex vivo. The combination of MDM2 and WEE1 inhibitors presents a promising therapeutic strategy for SRCC patients.

3. Discussion

SRCC is a unique form of adenocarcinoma in which the nucleus is pushed towards the edge of the cell because of the abundance of mucin in the cytoplasm. Gastric SRCC accounts for approximately 57 % of all SRCC cases and 16.8 % of all GC [27]. Moreover, the lack of effective drugs for SRCC is evidenced by the limited success rates of chemotherapy, targeted therapy, and immunotherapy, leading to poor outcomes [28].

Our study confirms that *MDM2* amplification is common in diffuse gastric cancer, aligning with previous findings [2,7]. The presence of the *MDM2* promoter SNP309 is associated with adverse outcomes in GC, whereas *MDM2* amplification in GC is associated with resistance to neoadjuvant treatment [29]. The study identified *MDM2* as a significant CNV gene in SRCC, with its increased expression linked to poor prognosis. The results suggest that MDM2 could be an effective target for SRCC treatment.

MDM2 inhibitors can interfere with the MDM2-p53 interaction, resulting in cell cycle arrest and tumor growth suppression [30]. However, the utility of MDM2 inhibitors is constrained due to dose-dependent toxicity and inconsistent p53 activation efficacy [13]. p53 can be activated by MDM2-TP53 inhibitors and induces DNA damage, thereby enhancing effectiveness of chemotherapy and radiotherapy [11,30–33]. Tumor growth is inhibited by cell cycle checkpoint inhibitors, such as CDK4/6 inhibitors, which specifically target the cell cycle [34]. The antitumor effect primarily results from inducing cell cycle arrest at the G2/M phase. Previous studies have demonstrated that SOX2 expression in prostate cancer induces resistance to nuclear hormone receptor signaling inhibition via the WEE1/CDK1 pathway [25]. This finding suggests that interfering with the cell cycle influences cancer progression. This study demonstrated that combining MDM2 inhibitors with either WEE1 or CHK1 inhibitors can greatly enhance p53 protein levels. This represents a promising strategy for effectively inhibiting tumor cells by activating p53. MDM2 negatively regulates E-cadherin protein levels via ubiquitination [18]. *CDH1* deletion occurs in 4 % of hereditary diffuse gastric cancer cases, leading to reduced E-cadherin expression [35,36]. The infrequent deletion of *CDH1* does not entirely account for the reduced expression of E-cadherin [9,37,38]. E-cadherin expression is often reduced in SRCC, even without *CDH1* mutations or deletions [39]. This study shows that MDM2 inhibitors alter SRCC morphology from signet-ring-like to spindle-like. Our study reveals that elevated MDM2 expression in SRCC modulates E-cadherin ubiquitination, providing insights into the mechanisms responsible for the reduced E-cadherin levels in SRCC.

The combination of MDM2 inhibitors with other drugs enhances antitumor efficacy synergistically [40]. Ida combined with Bcl-2 inhibitor venetoclax showed notable effectiveness in treating p53 wild-type acute myeloid leukemia (AML) [41]. The synergistic effect of combining MDM2 inhibitor with PD-1 blockade has shown significant antineoplastic activity in tumor models, regardless of *TP53* status [42]. Dual therapy comprising an MDM2 inhibitor and an FLT3 inhibitor is highly effective in treating FLT3-ITD-positive AML [43]. Ida can increase venetoclax sensitivity in relapsed/refractory AML, even in patients with *TP53* mutations [40,44]. However, the clinical effectiveness of a single application of an MDM2 inhibitor or FLT3 inhibitor is limited, and combination therapy can enhance clinical efficacy. In our study, we discovered a novel strategy that combines MDM2 inhibitors with either WEE1 or CHK1 inhibitors. This approach led to notable synthetic lethality in SRCC. A phase 2 study demonstrated a notable impact on patients with high-grade serous ovarian cancer when combining Ada with chemotherapeutics, suggesting potential clinical applications [45]. Importantly, the weight of the xenograft models derived from SNU668 and NUGC3 cells remained constant throughout the study, suggesting that the combination of Ada and MDM2 inhibitors was well-tolerated and had minimal harmful effects.

4. Conclusions

Collectively, our findings indicate that the use of MDM2 inhibition-induced morphological changes could potentially enhance the effects of G2/M checkpoint inhibitors, offering a promising strategy for combining treatments for SRCC.

Supplementary methods and figures

The supplementary methods and figures provide a comprehensive description of the materials and methodologies employed in this study.

CRediT authorship contribution statement

Dandong Luo: Writing – review & editing, Writing – original draft, Visualization, Validation, Software, Methodology, Investigation, Formal analysis, Data curation. **Huashe Wang:** Formal analysis, Data curation. **Jun Liu:** Software, Formal analysis. **Xiaochuan Chen:** Writing – review

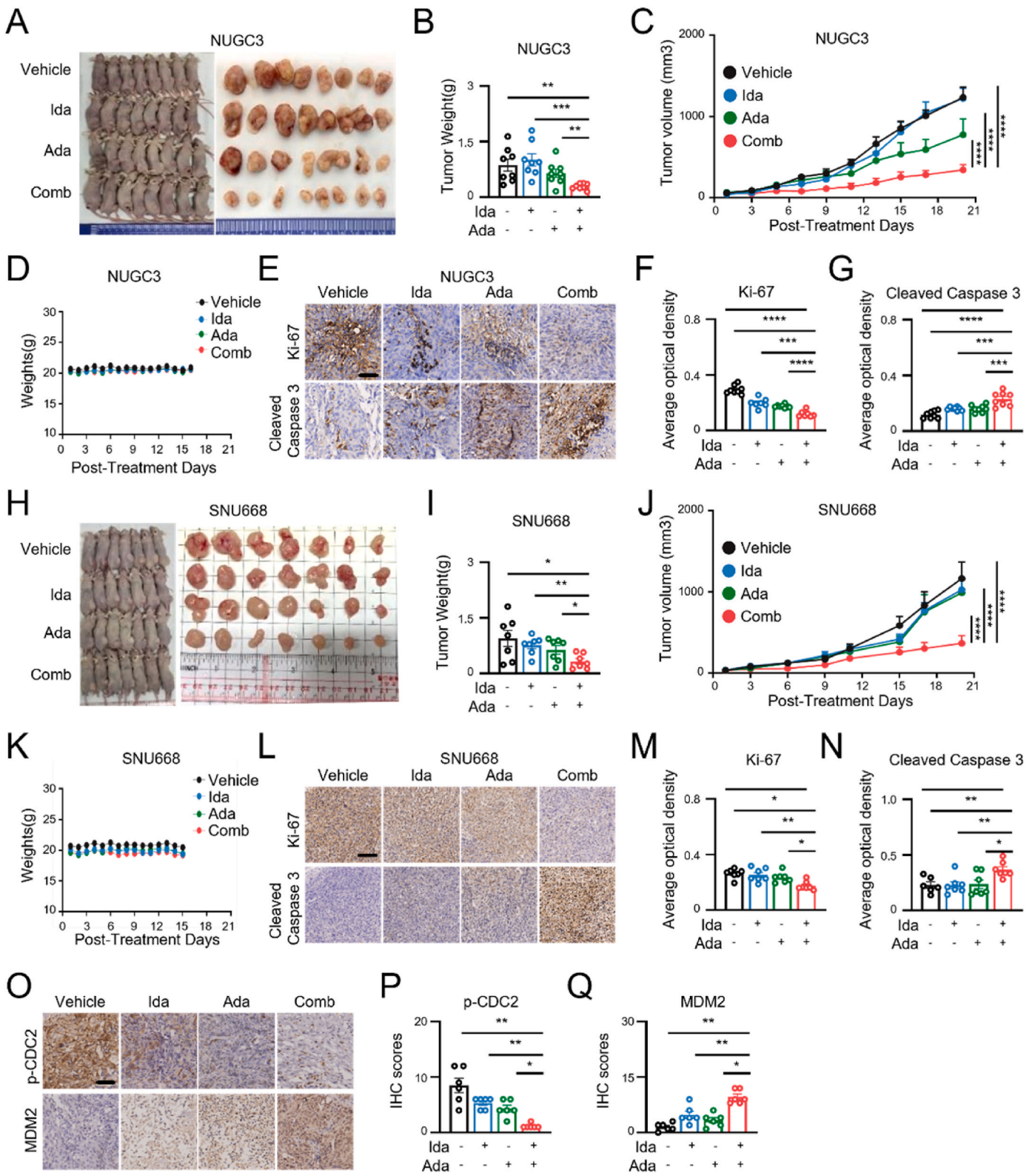

Fig. 4. Combination of MDM2 inhibitor and G2/M checkpoint inhibitors induces a synergistic antitumor effect in vivo and ex vivo (A–D) The representative image of tumor (A) tumor weights (B) growth curve of tumor volume (C) and body weights (D) treated with vehicle, Ida (37.5 mg/kg), Ada (150 mg/kg), or their combination in NUGC3 xenografts(n = 8). Error bars represent ± SEM. (E–G) The representative image(E), relative expression of Ki-67(F) and cleaved-caspase 3(G) of IHC in NUGC3 xenografts tumors (Scale bar, 100 μm). (H–K) The representative image of tumor (H) tumor weights (I) growth curve of tumor volume (J) and body weights (K) treated with vehicle, Ida (37.5 mg/kg), Ada (150 mg/kg), or their combination in SNU668 xenografts (n = 7). Error bars represent ± SEM. (L–N) The representative image (L), relative expression of Ki-67 (M) and cleaved-caspase 3 (N) of IHC in SNU668 xenografts tumors (Scale bar, 100 μm). (O–Q) The representative image (O), relative expression of p-CDC2 (M) and MDM2 (N) of IHC in SNU668 xenografts tumors (Scale bar, 100 μm).

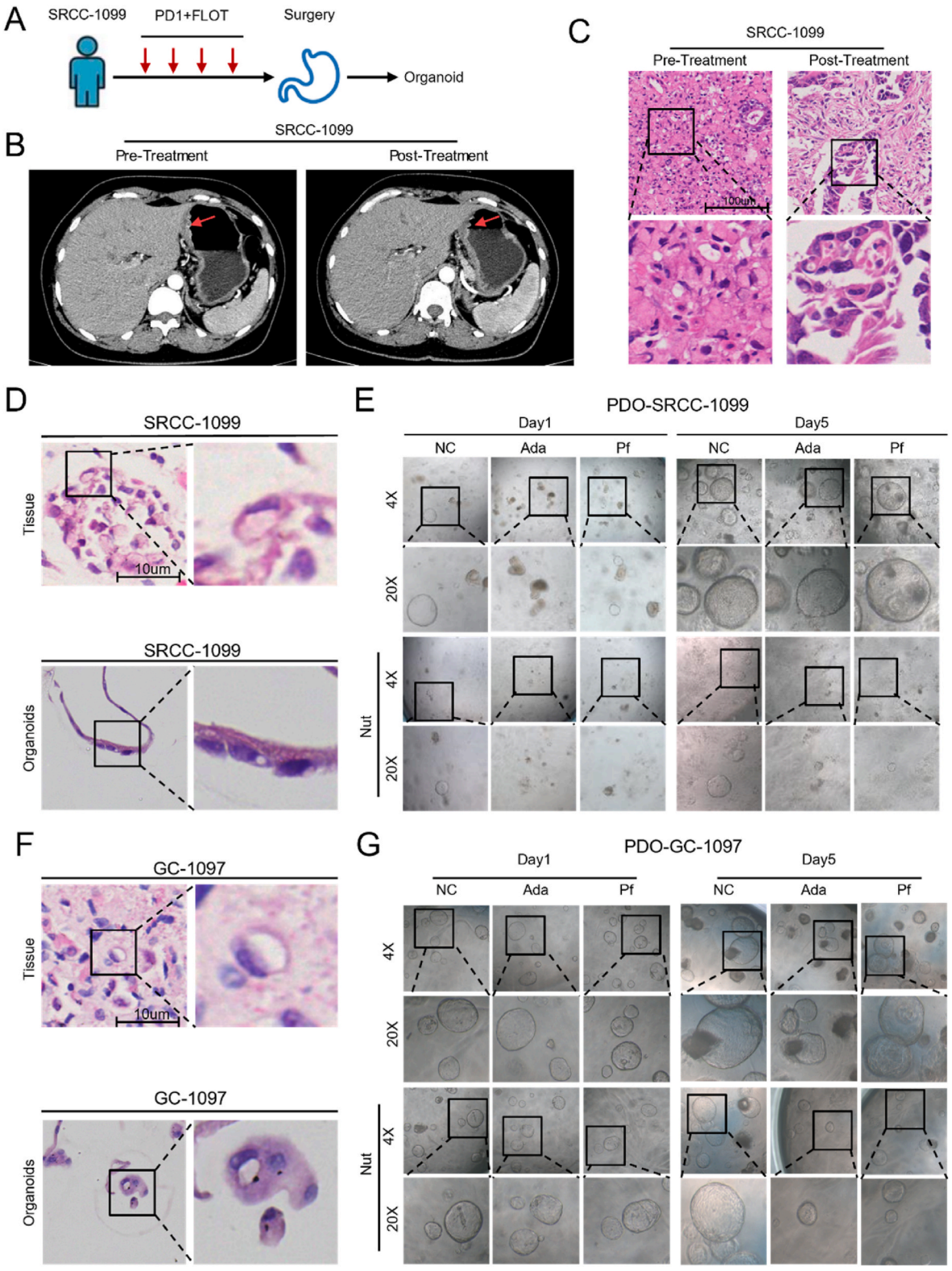

Fig. 5. Combination of MDM2 inhibitor and G2/M checkpoint inhibitors can induce a synergistic antitumor effect in patient-derived organoids (A) Schematic illustration of gastric SRCC patient derived organoids establishment. (B) Representative CT image of gastric SRCC patient (SRCC-1099) before and after neoadjuvant treatment, red arrow means the tumor location. (C) Representative H&E staining of SRCC-1099 tissues was performed both pre- and post-neoadjuvant treatment (Scale bar, 100 μm). (D) Representative H&E is staining of tissues and organoids derived from SRCC-1099 (Scale bar, 10 μm). (E) Representative image of SRCC-1099 treated with Nut, Ada, or Pf at an indicated concentration (Nut 10 μM, Ada 0.2 μM, Pf 0.2 μM) after 5 days of culture respectively (Scale bar = 200 μm). (F) Representative H&E is staining tissues and organoids derived from gastric poorly differentiated adenocarcinoma patient (GC-1097) (Scale bar, 10 μm). (G) Representative image of GC-1097 treated with Nut, Ada, or Pf at an indicated concentration (Nut 10 μM, Ada 0.2 μM, Pf 0.2 μM) after 5 days of culture respectively (Scale bar = 200 μm). (For interpretation of the references to color in this figure legend, the reader is referred to the Web version of this article.)

& editing, Data curation. **Yucheng Xu:** Methodology. **Yufan Liang:** Methodology. **Guannan Wang:** Methodology. **Jiabo Zheng:** Writing – review & editing. **Yonghe Chen:** Funding acquisition. **Xinyou Wang:** Funding acquisition. **Zhaoliang Yu:** Writing – review & editing, Writing – original draft, Validation, Supervision, Methodology, Funding acquisition. **Lei Lian:** Supervision, Resources, Funding acquisition, Conceptualization.

Ethics approval and consent to participate

This study complies with the Declaration of Helsinki and current ethical guidelines. The Ethical Committee of the Sixth Affiliated Hospital of Sun Yat-Sen University approved the study and waived the requirement for informed consent. No. 2021ZSLYEC-325).

Consent for publication

Not applicable.

Availability of data and materials

The complete set of analyzed data is included in this published article. You can request the original dataset from the corresponding author if needed.

Funding

This research received support from the Guangdong Provincial Clinical Research Center for Digestive Diseases program (No.).2020B1111170004), funded by the National Natural Science Foundation of China (No.82070684 and No.82203072), and the Guangdong Natural Science Fund for Outstanding Youth Scholars (No.2020B151502005) and the Bethune Ethicon Excellent Surgery Foundation (No.HZB-20190528-5), the Sixth Affiliated Hospital of Sun Yat-Sen University Clinical Research – '1010' Program (No.1010CG (2020)-02), National Key Clinical Discipline, Basic and Applied Basic Research Foundation of Guangdong Province (No.2021A1515111201, No.2022A1515111094 and No.2021A1515011630) and the Science and Technology Planning Project of Guangzhou (No.202201011111).

Declaration of competing interest

The authors declare that they have no known competing financial interests or personal relationships that could have appeared to influence the work reported in this paper.

Acknowledgements

The authors express their gratitude to all the patients who generously contributed samples for this study.

Appendix A. Supplementary data

Supplementary data to this article can be found online at https://doi.org/10.1016/j.canlet.2025.217500.

References

[1] Y. Li, Z. Zhu, F. Ma, L. Xue, Y. Tian, Gastric signet ring cell carcinoma: current management and future challenges, Cancer Manag. Res. 12 (2020) 7973–7981.
[2] A. Puccini, K. Poorman, F. Catalano, A. Seeber, R.M. Goldberg, M.E. Salem, A. F. Shields, M.D. Berger, F. Battaglin, R. Tokunaga, et al., Molecular profiling of signet-ring-cell carcinoma (SRCC) from the stomach and colon reveals potential new therapeutic targets, Oncogene 41 (26) (2022) 3455–3460.
[3] S. Taghavi, S.N. Jayarajan, A. Davey, A.I. Willis, Prognostic significance of signet ring gastric cancer, J. Clin. Oncol. 30 (28) (2012) 3493–3498.
[4] Z.M. Bamboat, L.H. Tang, E. Vinuela, D. Kuk, M. Gonen, M.A. Shah, M.F. Brennan, D.G. Coit, V.E. Strong, Stage-stratified prognosis of signet ring cell histology in patients undergoing curative resection for gastric adenocarcinoma, Ann. Surg Oncol. 21 (5) (2014) 1678–1685.
[5] T. Voron, M. Messager, A. Duhamel, J. Lefevre, J.Y. Mabrut, D. Goere, B. Meunier, C. Brigand, A. Hamy, O. Glehen, et al., Is signet-ring cell carcinoma a specific entity among gastric cancers? Gastric Cancer 19 (4) (2016) 1027–1040.
[6] A. Puccini, K. Poorman, F. Catalano, A. Seeber, R.M. Goldberg, M.E. Salem, A. F. Shields, M.D. Berger, F. Battaglin, R. Tokunaga, et al., Molecular profiling of signet-ring-cell carcinoma (SRCC) from the stomach and colon reveals potential new therapeutic targets, Oncogene 41 (26) (2022) 3455–3460.
[7] Y. Shu, W. Zhang, Q. Hou, L. Zhao, S. Zhang, J. Zhou, X. Song, Y. Zhang, D. Jiang, X. Chen, et al., Prognostic significance of frequent CLDN18-ARHGAP26/6 fusion in gastric signet-ring cell cancer, Nat. Commun. 9 (1) (2018) 2447.
[8] L. O'Driscoll, When E-cadherin becomes unstuck in cancer, N. Engl. J. Med. 383 (9) (2020) 871–873.
[9] K. Yamaguchi, T. Yoshihiro, H. Ariyama, M. Ito, M. Nakano, Y. Semba, J. Nogami, K. Tsuchihashi, T. Yamauchi, S. Ueno, et al., Potential therapeutic targets discovery by transcriptome analysis of an in vitro human gastric signet ring carcinoma model, Gastric Cancer 25 (5) (2022) 862–878.
[10] X. Cui, X. Shang, J. Xie, C. Xie, Z. Tang, Q. Luo, C. Wu, G. Wang, N. Wang, K. He, et al., Cooperation between IRTKS and deubiquitinase OTUD4 enhances the SETDB1-mediated H3K9 trimethylation that promotes tumor metastasis via suppressing E-cadherin expression, Cancer Lett. 575 (2023) 216404.
[11] D.D. Fang, Q. Tang, Y. Kong, T. Rong, Q. Wang, N. Li, X. Fang, J. Gu, D. Xiong, Y. Yin, et al., MDM2 inhibitor APG-115 exerts potent antitumor activity and synergizes with standard-of-care agents in preclinical acute myeloid leukemia models, Cell Death Discov 7 (1) (2021) 90.
[12] I. Sahin, S. Zhang, A. Navaraj, L. Zhou, D. Dizon, H. Safran, W.S. El-Deiry, AMG-232 sensitizes high MDM2-expressing tumor cells to T-cell-mediated killing, Cell Death Discov 6 (2020) 57.
[13] M. Konopleva, G. Martinelli, N. Daver, C. Papayannidis, A. Wei, B. Higgins, M. Ott, J. Mascarenhas, M. Andreeff, MDM2 inhibition: an important step forward in cancer therapy, Leukemia 34 (11) (2020) 2858–2874.
[14] K. Kojima, S.M. Kornblau, V. Ruvolo, A. Dilip, S. Duvvuri, R.E. Davis, M. Zhang, Z. Wang, K.R. Coombes, N. Zhang, et al., Prognostic impact and targeting of CRM1 in acute myeloid leukemia, Blood 121 (20) (2013) 4166–4174.
[15] Z. Tang, B. Kang, C. Li, T. Chen, Z. Zhang, GEPIA2: an enhanced web server for large-scale expression profiling and interactive analysis, Nucleic Acids Res. 47 (W1) (2019) W556–w560.
[16] B. Győrffy, Integrated analysis of public datasets for the discovery and validation of survival-associated genes in solid tumors, Innovation 5 (3) (2024) 100625.
[17] J. Barretina, G. Caponigro, N. Stransky, K. Venkatesan, A.A. Margolin, S. Kim, C. J. Wilson, J. Lehár, G.V. Kryukov, D. Sonkin, et al., The Cancer Cell Line Encyclopedia enables predictive modelling of anticancer drug sensitivity, Nature 483 (7391) (2012) 603–607.
[18] J.Y. Yang, C.S. Zong, W. Xia, Y. Wei, M. Ali-Seyed, Z. Li, K. Broglio, D.A. Berry, M. C. Hung, MDM2 promotes cell motility and invasiveness by regulating E-cadherin degradation, Mol. Cell Biol. 26 (19) (2006) 7269–7282.
[19] C. Ma, N. Zhang, T. Wang, H. Guan, Y. Huang, L. Huang, Y. Zheng, L. Zhang, L. Han, Y. Huo, et al., Inflammatory cytokine-regulated LNCPTCTS suppresses thyroid cancer progression via enhancing Snail nuclear export, Cancer Lett. 575 (2023) 216402.
[20] R.M. de Queiroz, G. Efe, A. Guzman, N. Hashimoto, Y. Kawashima, T. Tanaka, A. K. Rustgi, C. Prives, Mdm2 requires Sprouty4 to regulate focal adhesion formation and metastasis independent of p53, Nat. Commun. 15 (1) (2024) 7132.
[21] W. Wang, J.W. Cheng, J.J. Qin, B. Hu, X. Li, B. Nijampatnam, S.E. Velu, J. Fan, X. R. Yang, R. Zhang, MDM2-NFAT1 dual inhibitor, MA242: effective against hepatocellular carcinoma, independent of p53, Cancer Lett. 459 (2019) 156–167.
[22] R. Riscal, E. Schrepfer, G. Arena, M.Y. Cissé, F. Bellvert, M. Heuillet, F. Rambow, E. Bonneil, F. Sabourdy, C. Vincent, et al., Chromatin-bound MDM2 regulates serine metabolism and redox homeostasis independently of p53, Mol Cell 62 (6) (2016) 890–902.
[23] T.J. Peat, S.M. Gaikwad, W. Dubois, N. Gyabaah-Kessie, S. Zhang, S. Gorjifard, Z. Phyo, M. Andres, V.K. Hughitt, R.M. Simpson, et al., Drug combinations identified by high-throughput screening promote cell cycle transition and upregulate Smad pathways in myeloma, Cancer Lett. 568 (2023) 216284.
[24] X. Lin, D. Chen, C. Zhang, X. Zhang, Z. Li, B. Dong, J. Gao, L. Shen, Augmented antitumor activity by olaparib plus AZD1775 in gastric cancer through disrupting DNA damage repair pathways and DNA damage checkpoint, J. Exp. Clin. Cancer Res. 37 (1) (2018) 129.
[25] A. Williams, L. Gutgesell, L. de Wet, P. Selman, A. Dey, M. Avineni, I. Kapoor, M. Mendez, R. Brown, S. Lamperis, et al., SOX2 expression in prostate cancer drives resistance to nuclear hormone receptor signaling inhibition through the WEE1/CDK1 signaling axis, Cancer Lett. 565 (2023) 216209.
[26] R. Yang, Y. Yu, Patient-derived organoids in translational oncology and drug screening, Cancer Lett. 562 (2023) 216180.
[27] M.G.K. Benesch, A. Mathieson, Epidemiology of signet ring cell adenocarcinomas, Cancers 12 (6) (2020).
[28] N.L.L. Phoo, P. Dejkriengkraikul, P. Khaw-On, S. Yodkeeree, Transcriptomic profiling reveals AKR1C1 and AKR1C3 mediate cisplatin resistance in signet ring cell gastric carcinoma via autophagic cell death, Int. J. Mol. Sci. 22 (22) (2021).
[29] Z. Li, X. Gao, X. Peng, M.J. May Chen, Z. Li, B. Wei, X. Wen, B. Wei, Y. Dong, Z. Bu, et al., Multi-omics characterization of molecular features of gastric cancer correlated with response to neoadjuvant chemotherapy, Sci. Adv. 6 (9) (2020) eaay4211.

[30] L.T. Vassilev, B.T. Vu, B. Graves, D. Carvajal, F. Podlaski, Z. Filipovic, N. Kong, U. Kammlott, C. Lukacs, C. Klein, et al., In vivo activation of the p53 pathway by small-molecule antagonists of MDM2, Science 303 (5659) (2004) 844–848.
[31] H. Yi, X. Yan, Q. Luo, L. Yuan, B. Li, W. Pan, L. Zhang, H. Chen, J. Wang, Y. Zhang, et al., A novel small molecule inhibitor of MDM2-p53 (APG-115) enhances radiosensitivity of gastric adenocarcinoma, J. Exp. Clin. Cancer Res. 37 (1) (2018) 97.
[32] H. Wang, S. Cai, B.J. Bailey, M. Reza Saadatzadeh, J. Ding, E. Tonsing-Carter, T. M. Georgiadis, T. Zachary Gunter, E.C. Long, R.E. Minto, et al., Combination therapy in a xenograft model of glioblastoma: enhancement of the antitumor activity of temozolomide by an MDM2 antagonist, J. Neurosurg. 126 (2) (2017) 446–459.
[33] L. Chen, S. Agrawal, W. Zhou, R. Zhang, J. Chen, Synergistic activation of p53 by inhibition of MDM2 expression and DNA damage, Proc Natl Acad Sci U S A 95 (1) (1998) 195–200.
[34] C. Wang, T. Wang, K.J. Li, L.H. Hu, Y. Li, Y.Z. Yu, T. Xie, S. Zhu, D.J. Fu, Y. Wang, et al., SETD4 inhibits prostate cancer development by promoting H3K27me3-mediated NUPR1 transcriptional repression and cell cycle arrest, Cancer Lett. 579 (2023) 216464.
[35] J. Xiao, H. Li, F. Xue, Z. Luo, Y. Pang, Prenatal diagnosis of hereditary diffuse gastric cancer: a case report, BMC Pregnancy Childbirth 23 (1) (2023) 488.
[36] B. Humar, V. Blair, A. Charlton, H. More, I. Martin, P. Guilford, E-cadherin deficiency initiates gastric signet-ring cell carcinoma in mice and man, Cancer Res. 69 (5) (2009) 2050–2056.
[37] H. Murakami, H. Nakanishi, H. Tanaka, S. Ito, K. Misawa, Y. Ito, Y. Ikehara, E. Kondo, Y. Kodera, Establishment and characterization of novel gastric signet-ring cell and non signet-ring cell poorly differentiated adenocarcinoma cell lines with low and high malignant potential, Gastric Cancer 16 (1) (2013) 74–83.
[38] M.E. Börger, M.J. Gosens, J.W. Jeuken, L.C. van Kempen, C.J. van de Velde, J. H. van Krieken, I.D. Nagtegaal, Signet ring cell differentiation in mucinous colorectal carcinoma, J. Pathol. 212 (3) (2007) 278–286.
[39] M. Nikaido, N. Kakiuchi, S. Miyamoto, T. Hirano, Y. Takeuchi, T. Funakoshi, A. Yokoyama, T. Ogasawara, Y. Yamamoto, A. Yamada, et al., Indolent feature of Helicobacter pylori-uninfected intramucosal signet ring cell carcinomas with CDH1 mutations, Gastric Cancer 24 (5) (2021) 1102–1114.
[40] E.S. Wang, MDM2 and BCL-2: to p53 or not to p53? Blood 141 (11) (2023) 1237–1238.
[41] C. Lehmann, T. Friess, F. Birzele, A. Kiialainen, M. Dangl, Superior anti-tumor activity of the MDM2 antagonist idasanutlin and the Bcl-2 inhibitor venetoclax in p53 wild-type acute myeloid leukemia models, J. Hematol. Oncol. 9 (1) (2016) 50.
[42] D.D. Fang, Q. Tang, Y. Kong, Q. Wang, J. Gu, X. Fang, P. Zou, T. Rong, J. Wang, D. Yang, Y. Zhai, MDM2 inhibitor APG-115 synergizes with PD-1 blockade through enhancing antitumor immunity in the tumor microenvironment, J Immunother Cancer 7 (1) (2019) 327.
[43] K. Seipel, M.A.T. Marques, C. Sidler, B.U. Mueller, T. Pabst, MDM2- and FLT3-inhibitors in the treatment of FLT3-ITD acute myeloid leukemia, specificity and efficacy of NVP-HDM201 and midostaurin, Haematologica 103 (11) (2018) 1862–1872.
[44] N.G. Daver, M. Dail, J.S. Garcia, B.A. Jonas, K.W.L. Yee, K.R. Kelly, N. Vey, S. Assouline, G.J. Roboz, S. Paolini, et al., Venetoclax and idasanutlin in relapsed/refractory AML: a nonrandomized, open-label phase 1b trial, Blood 141 (11) (2023) 1265–1276.
[45] S. Lheureux, M.C. Cristea, J.P. Bruce, S. Garg, M. Cabanero, G. Mantia-Smaldone, A.B. Olawaiye, S.L. Ellard, J.I. Weberpals, A.E. Wahner Hendrickson, et al., Adavosertib plus gemcitabine for platinum-resistant or platinum-refractory recurrent ovarian cancer: a double-blind, randomised, placebo-controlled, phase 2 trial, Lancet 397 (2021) 281–292, 10271.